International Conference on Control, Engineering & Information Technology (CEIT'13)
Proceedings Engineering & Technology - Vol.4, pp. 78-82,2013

Vector control of an induction machine

H.othmani[#1], D.Mezghani[#2], A.Mami[#3]
laboratory of Analysis and Control Systems, Department of Electric Engineering
National School of Engineering of Tunis
BP 37, Belvedere, Tunis 1002, Tunisia
[1] hiochem1@gmail.com, [2] dhafer.mezghanni@gmail.com, [3] abdelkader.mami@gmail.com

***Abstract*——** **In this electronic document, we study the modeling and the control of an induction machine. The proposed system outputs through a Pulse Width Modulation inverter checked up at continuous output by a Vector control in order to obtain a maximum energetic efficiency. The results of various simulations of all the chain of conversion, carried out under MTLAB/Simulink software, made it possible to evaluate the performances of the proposed system.**

Keywords——*: Induction machine; simulation; Vector control; Modeling; PWM;*

I. INTRODUCTION

To optimize the functioning of the induction machine, we must choose a control that can deliver the maximum power output (optimal performance) and reduce the harmful effects due to load disturbances. Vector control with rotor flux oriented control is a reliable control. It has the advantage of eliminating the influence of the leakage reactance rotor and stator, which provides better results. In this strategy we try to emulate the operation of the induction machine to that of a DC machine with independent excitation, where there is a natural decoupling between the excitation current and the armature current. This decoupling allows for a very fast response of torque. In this paper, we presented the model of an induction machine and the vector control of this machine. We will then quote the simulation results of our system and comment. The remainder of the paper is organized as follows: Section (2) focuses on the modeling of the machine. Section (3) emphasizes on the method of control of this machine. Section (4) is reserved for the result of simulation of our system.

II. MODELLING OF INDUCTION MACHINE

The induction motor is the engine most used worldwide. The most economical and the most common electric motors is characterized by a simple and robust design. An induction machine can be represented by three identical to the stator windings.

The equation of the machine is then written in the following form:

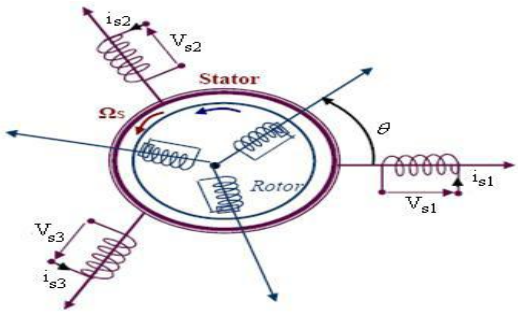

Fig. 1. Layout spatial phase stator and rotor

$$[V_{s123}] = [R_s][I_{s123}] + \frac{d}{dt}[\varphi_{s123}] \quad (1)$$

$$[V_{r123}] = [R_r][I_{r123}] + \frac{d}{dt}[\varphi_{r123}] = 0 \quad (2)$$

Noting that:

$$\begin{aligned} [\varphi_{r123}] &= [\varphi_{r1} \quad \varphi_{r2} \quad \varphi_{r3}]^t \\ [I_{r123}] &= [I_{r1} \quad I_{r2} \quad I_{r3}]^t \\ [V_{r123}] &= [0 \quad 0 \quad 0]^t \end{aligned} \quad (3)$$

$$\begin{aligned} [V_{s123}] &= [V_{s1} \quad V_{s2} \quad V_{s3}]^t \\ [\varphi_{s123}] &= [\varphi_{s1} \quad \varphi_{s2} \quad \varphi_{s3}]^t \\ [I_{s123}] &= [I_{s1} \quad I_{s2} \quad I_{s3}]^t \end{aligned} \quad (4)$$

$$[R_s] = diag(R_s); \quad [R_r] = diag(R_r) \quad (5)$$

Previous equations brings us back to matrix equations nonlinear and high dimensional not easily exploitable. To overcome this problem we use the transformation of PARK (detailed in (II.B)). We apply a Park transformation P [θ_s] to the stator and another **P**[θ_s-θ] to the rotor, where θ_s is the angle of the marker of the stator. θ is the electric angle related to the mechanical position of the motor θ_m by relationship $\theta = np\ \theta_m$

So (1) and (2) becomes:

$$[V_{sdq}] = [R_s][I_{sdq}] + \frac{d}{dt}[\varphi_{sdq}] \tag{6}$$

$$[V_{rdq}] = [R_r][I_{rdq}] + \frac{d}{dt}[\varphi_{rdq}] = 0 \tag{7}$$

Noting that:

$$\begin{aligned} [\varphi_{rdq}] &= [\varphi_{rd} \quad \varphi_{rq}]^t \\ [I_{rdq}] &= [I_{rd} \quad I_{rq}]^t \\ [V_{rdq}] &= [0 \quad 0]^t \end{aligned} \tag{8}$$

$$\begin{aligned} [V_{sdq}] &= [V_{sd} \quad V_{sq}]^t \\ [\varphi_{sdq}] &= [\varphi_{rd} \quad \varphi_{rq}]^t \\ [I_{sdq}] &= [I_{sd} \quad I_{sq}]^t \end{aligned} \tag{9}$$

$$\varphi_{ds} = L_s i_{ds} + L_m i_{dr} \qquad \varphi_{qs} = L_s i_{qs} + L_m i_{qr}$$

$$\varphi_{dr} = L_s i_{dr} + L_m i_{dr} \qquad \varphi_{qr} = L_s i_{qr} + L_m i_{qr} \tag{10}$$

$$L_s = l_s + L_m \qquad L_r = l_r + L_m \tag{11}$$

$$P[\theta_s]\frac{dP[\theta s]}{dt} = \omega_s \begin{bmatrix} 0 & -1 \\ 1 & 0 \end{bmatrix} \tag{12}$$

$$P[\theta_s - \theta]\frac{dP[\theta s - \theta]}{dt} = \omega_r \begin{bmatrix} 0 & -1 \\ 1 & 0 \end{bmatrix} \tag{13}$$

$$\omega_s = \frac{d\theta s}{dt} \tag{14}$$

$$\omega_r = \omega_s - \omega = \frac{d(\theta_s - \theta)}{dt} \tag{15}$$

Based on the foregoing, the corresponding electrical circuit q-axis is shown in Fig. 2. The circuit of the axis is almost the same. Just we change the variables with those of the b axis and we invert the polarity of the pulse-related sources.

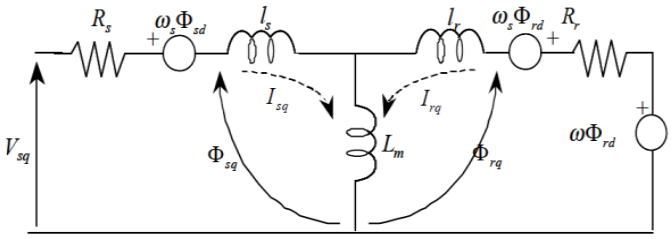

Fig. 2. Equivalent circuit of the q-axis of a two-phase asynchronous machine.

The park model leads to several expressions of the electromagnetic torque cem we retain:

$$C_{em} = n_p \frac{L_m}{L_r} (i_{qs}\ \Phi_{dr} - i_{ds}\ \Phi_{qr}) \tag{16}$$

III. CONTROL OF INDUCTION MACHINE

The vector control is, in each period of operation of the inverter, an opening or closing of the power switches in order to create a magnetic field to the electric machine whose magnitude and direction are to meet the optimal speed setpoints and couple. We try to emulate the operation of the induction machine to that of a DC machine with independent excitation, where there is a natural decoupling between the excitation current and the armature current.

A. Structure of the vector control

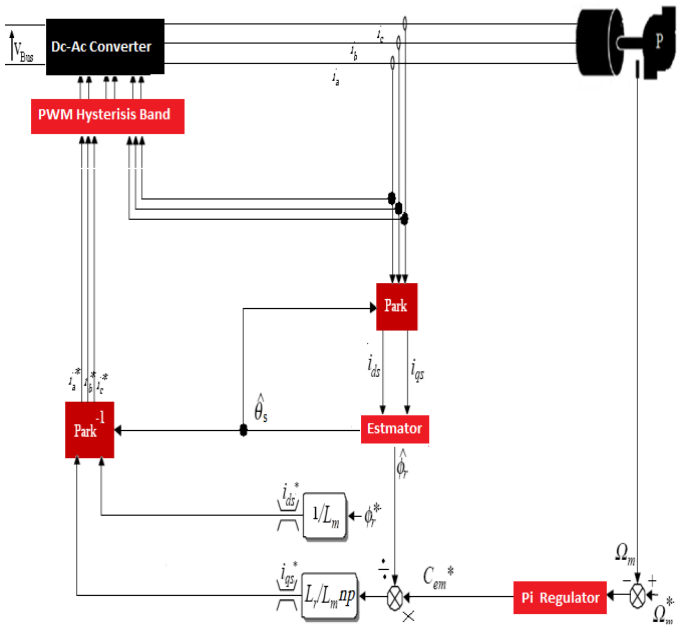

Fig. 3. Block diagram of vector control.

The electromagnetic torque is given by:

$$C_{em} = n_p \frac{L_m}{L_r} \hat{\Phi}_r \, i_{qs} \tag{17}$$

Noting that:

$\hat{\Phi}_r$ is the flow estimated by the estimation block.

So we see that the electromagnetic torque is based on a single current (that is the purpose of vector control).

The rotor flux is estimated from I_{ds}, the actual stator current measurement after the Park transformation.

Where:

$$\hat{\Phi}_r = \frac{L_m \, i_{ds}}{1 + s.T_r} \tag{18}$$

$$T_r = \frac{L_r}{R_r} \tag{19}$$

The pulsation angular θ_s Benchmark dq-axis relative to a stator phase. It is defined by the following equation :

$$\hat{\omega}_s = \hat{\omega}_m + \hat{\omega}_r = n_p \Omega_m + \frac{L_m}{T_r} \frac{i_{qs}}{\hat{\Phi}_r} \tag{20}$$

$$\hat{\theta}_s = \int \hat{\omega}_s \, dt \tag{21}$$

$\hat{\omega}_r$ is the electrical rotor pulse

$\hat{\omega}_m$ is the mechanical rotor pulse

B. *Park Transformation*

The The Park transformation allows us to transform the variables of a three-phase system in a two-equivalent-phase.

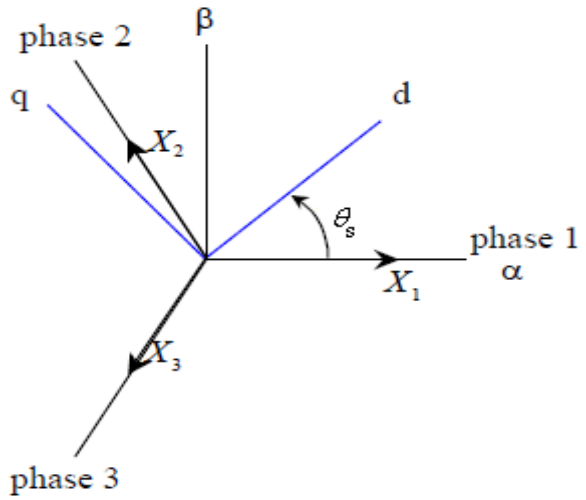

Fig. 4. Relationship between a phase and a two-phase equivalent.

This transformation is defined by

$$\begin{bmatrix} X_d \\ X_q \\ X_0 \end{bmatrix} = P(\theta_s) \begin{bmatrix} X_1 \\ X_2 \\ X_3 \end{bmatrix} \tag{22}$$

$$P(\theta_s) = \sqrt{\frac{2}{3}} \begin{bmatrix} \cos\theta_s & \cos\left(\theta_s - \frac{2\pi}{3}\right) & \cos\left(\theta_s + \frac{2\pi}{3}\right) \\ -\sin\theta_s & -\sin\left(\theta_s - \frac{2\pi}{3}\right) & -\sin\left(\theta_s + \frac{2\pi}{3}\right) \\ \sqrt{\frac{1}{2}} & \sqrt{\frac{1}{2}} & \sqrt{\frac{1}{2}} \end{bmatrix} \tag{23}$$

$$\begin{bmatrix} x_a \\ x_b \\ x_c \end{bmatrix} = P^T(\theta_s) \begin{bmatrix} x_d \\ x_q \\ x_h \end{bmatrix} \tag{24}$$

$$M(\theta_s) = \begin{bmatrix} \cos\theta_s & \sin\theta_s \\ -\sin\theta_s & \cos\theta_s \end{bmatrix} \tag{25}$$

$$P(0) = \sqrt{\frac{2}{3}} \begin{bmatrix} 1 & \frac{-1}{2} & \frac{-1}{2} \\ 0 & \frac{-\sqrt{3}}{2} & \frac{\sqrt{3}}{2} \end{bmatrix} \tag{26}$$

P (0) has a special character, it does not depend on the angle θ_s, it forms a constant linear transformation is the transformation Concordia, which is not the case of P (θ_s) In addition, it is invertible, we can then more easily mathematical operations in the same way for the two vectors that lie.

C. *Speed Control*

To control the speed, we chose a Proportional Integral correction. We have the following transfer function:

$$\frac{\Omega_m}{C_{em}} = \frac{1}{R_{nlp} + J\,s} \tag{27}$$

With R_{nlp} the losses in the shaft of the pump, the PI regulator transfer function, permitting to eliminate the mechanical time-constant and to zeroed the error.

$$R_{nlp} = C_2 \Omega_m + C_1 \tag{28}$$

D. PWM (Puls Width Modulation) Hysteresis Band

The method of the hysteresis band allows the switching of the interrupter when the error between the signal and the setpoint exceeds a fixed amplitude. Indeed, in the modulation of the stator currents are hysteresis compared with reference currents within a hysteresis band. The controller generates sinusoidal reference current of the desired frequency, which are then compared to the current resulting from motor stator. If the current exceeds the upper limit of the hysteresis band, the upper switch arm switch is turned off and the lower switch is activated.

As a result, the current starts to decay. If the current exceeds the lower limit of the hysteresis band, the lower switch arm inverter is turned off and the upper enabled. As a result, the current returns to the hysteresis band. Thus, the actual current is forced to follow the reference current in the hysteresis band. Figure 2.5 illustrates the principle of operation of a regulator with hysteresis.

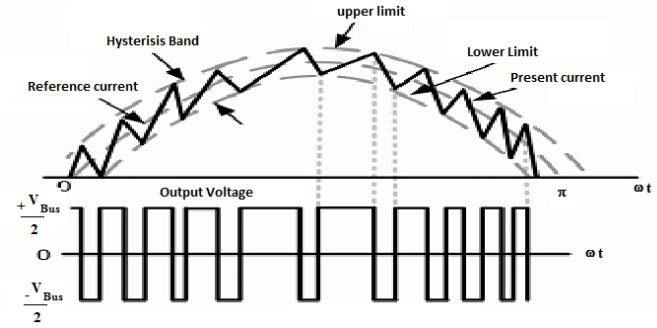

Fig. 5. Principle of operating a hysteresis controller

This command is most commonly used because of its ease of use and robustness. In fact, this strategy provides satisfactory control current without requiring extensive knowledge of the system model to control or settings. Fig. 6 presents the principle of establishing a first error signal, the difference between the reference currents i_{sabc} *, and after the inverter current i_{sabc}. This error is then compared to a template called hysteresis band to fix the orders for controlling the switches.

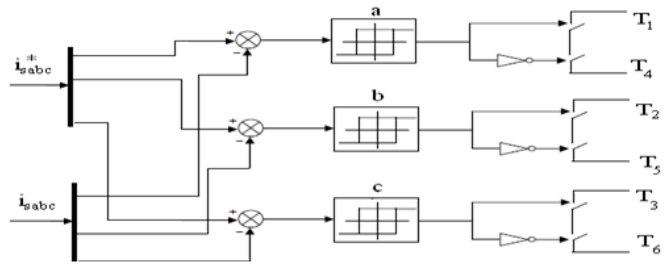

Fig. 6. Hhysteresis Band Regulator

IV. SIMULATION RESULT

The operation of the entire environment was simulated under MATLAB ®, Simulink ®. The speed and flux references are respectively: X_{m0} = 300 rd/s = 2866 rpm, U_{r0} = 0.932 Wb.

The input voltage is 380V.

The Asynchronous motor-pump is characterized by:

Numbers of poles: 2,

Nominal voltage: 230/400 V,

Nominal current: 1.6 A,

Nominal power output: 750 W,

Nominal speed: 2866 rpm,

Nominal frequency: 50 Hz,

Total moment of inertia, J: 0.0015 kg m2,

Constant of pump torque, K_r: 2.772 kg m2 rd_1

Coefficient of friction, F: 3.44 · 10_5 kg m2 s_1,

Stator resistance, Rs: 10.621 Ω,

Rotor resistance, R_R: 7Ω,

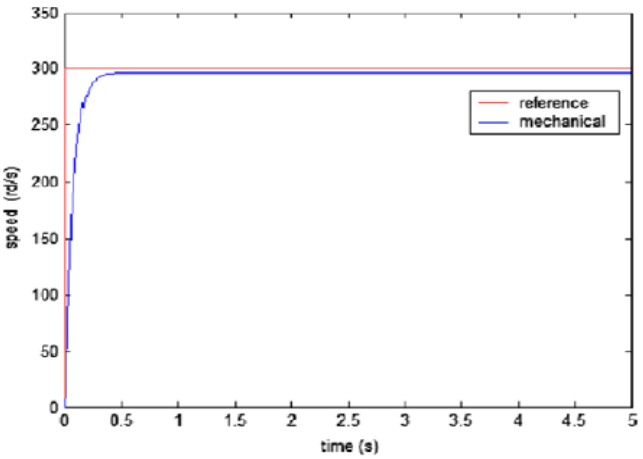

(1) Fig. 7. Simulation response of speed (1)

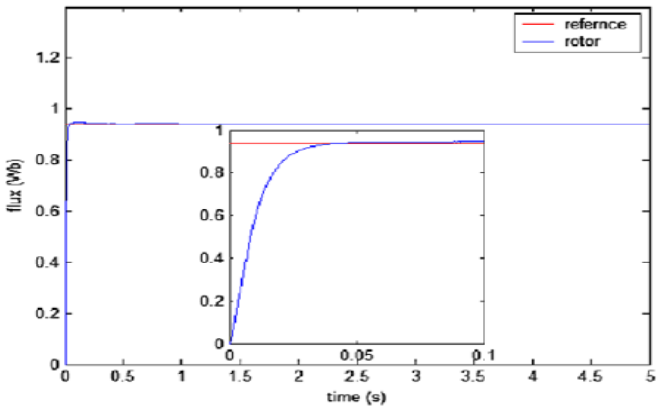

Fig. 8. Simulation reponse of flux

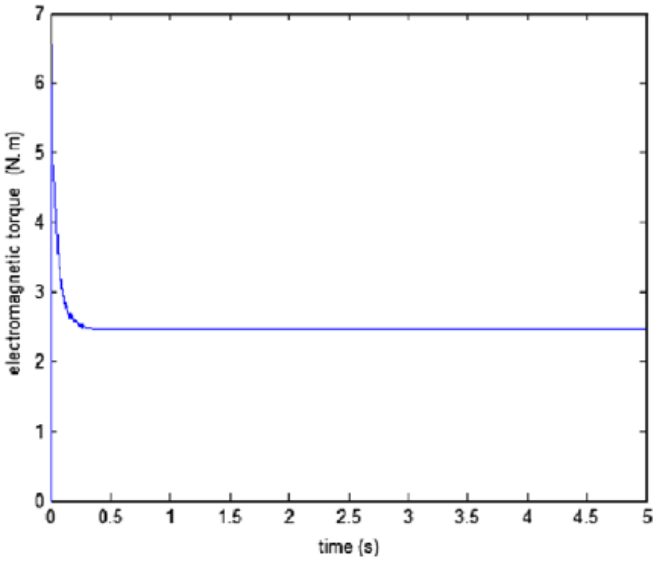

Fig. 9. Simulation reponse of Torque

V. CONCLUSIONS

In this paper, we have developed mathematical models of our Syteme. Law control system has been detailed. The results of various simulations have performed to validate the proposed mathematical models.

REFERENCES

[1] L.Charaabi, E.Monmasson, and I.Slama-BelKodja, "Presentation of an efficient design methodologiy to develop IP-core functions For control systems : Application to the Design of an antiwindup PI controller ", IEEE IECON,Sevilla,Spain,Nov.(2002).

[2] M. Turki, J. Belhaj and X.Roboam "Control strategie of an autonomous desalination unit fed by PV-Wind hybrid system without battery storage ", J.Electrical Systeme 4-2 (2008).

[3] R. Xavier, "Variateur de vitesse pour machine asynchrone developpement des lois de commande robuste", these INPT, (1991).

[4] D. Mezghanni D, Andoulsi R, Mami A and Dauphin-Tanguy G, " Bond graph modelling of a photovoltaic system feeding an induction motor-pump", Simulation Modelling Practice and Theory voln°15, pp. 1224–1238, (2007).

[5] S. Belakehal, A. Bentounsi, M. Merzoug and H. Benalla "Modélisation Modélisation et commande d'une génératrice Synchrone à aimants permanents dédiée à la conversion de l'énergie éolienne ", Revue des Energies Renouvelables Vol. 13 N°1 Mars (2010)

[6] A. Boumaaraf, M. D. Draou and S. A. Chikhi " Un Nouveau Concept de la Commande PWM Destiné au Système de Pompage Photovoltaïque ", Revue des Energies Renouvelables Vol. 05, (2002).

[7] M. Arrouf, N. Bouguechal, "Vector control of an induction motor fed by a photovoltaic generator ", Applied Energy 74 (2003) 159–167.

[8] V.N. Madansure, "Bond graph modelling and simulation of spice-pounding machines fed from a photovoltaic source", InternationalJournal of energy research 21 (1996) 683–694.

[9] L.Baghli " Contribution à la commande de la machine asynchrone,utilisation de la logique floue,des reseaux de neurones et des algorithmes génitiques ", Phd,FS Nancy1, (1999).

[10] I.Vechui " Modelisation et analyse de l'integration des energies renouvlables dans un reseau autonome ", Phd,Université du Havre, (2005).

[11] G. Gandanegara "Methodologie de conception systemique en génie Electrique à l'aide de l'outil Bond Graph Application à une chaine de traction ferroviaire ", Phd, UMR INP Toulouse, (2003).

[12] M.F. Mimouni, M.N.Mansouri., B.Benghanem, M.Annabi"Vectorial commandof an asynchronous motor fedby a photovoltaic generator ", Renewable Energy 29 (2004) 433–442.

[13] A.Ghazel, "Controle vectoriel numerique d'une machine asynchrone alimentee par un onduleur MLI", Phd ENIT, Tunis, (1996).